Fermi National Accelerator Laboratory

FN-523

Acceptances for Charm Photoproduction*

J. Busenitz
Fermi National Accelerator Laboratory
P.O. Box 500
Batavia, Illinois 60510

October 1, 1989

* Talk given at "Physics at Fermilab in the 1990's," Breckenridge, Colorado, August 15-24, 1989.

Operated by Universities Research Association Inc. under contract with the United States Department of Energy

Acceptances for Charm Photoproduction

J. Busenitz

1 October 1989

I. Introduction

In order to provide a point of reference for estimating the acceptances of current charm photoproduction experiments and for understanding acceptance losses, I have made a rough measurement of the acceptance of the E687 detector for the photoproduction of D^+ decaying into $K\pi\pi$ and for Λ_c decaying into $pK\pi$. The choice of the relatively long-lived D^+ and the relatively short-lived Λ_c states was made in order to indicate the range of acceptances obtained after applying the cuts-critical to background suppression-on the separation between the primary production vertex and the secondary decay vertex. The decay modes chosen are the so-called "golden" decay modes, the acceptances for which, excluding vertex cuts, are probably close to the mean of the acceptances of the all-charged decay modes. Clearly the acceptances obtained depend on the E687 detector, the production model used for the simulation, and the reconstruction program, and so I will attempt to provide the relevant details on these below.

II. The Monte Carlo

We first note some details of the Monte Carlo program. The charm quark pair was produced according to the photon-gluon fusion model with the photon drawn from a bremmstrahlung spectrum between 50 and 350 GeV and the gluon structure function taken to depend on (1-x) as $(1\text{-}x)^5$. Dressing of the charm quarks into hadrons assumed the hard fragmentation function $\delta(z-1)$. (The choice of this overly hard fragmentation function was made in order to broaden the distributions in momentum and x_F. If a more realistic fragmentation function is chosen, e.g. the Petersen function, the integrated acceptances after geometric cuts and particle ID cuts are scaled up by a factor of about 1.1 relative to what's quoted below.) The decays of the hadrons were generated according to phase space. Finally, multiple scattering of the charged particles in the detector material, as well as K and π decays, were fully simulated.

Figure 1 shows generated distributions obtained from this Monte Carlo: Fig. 1a is the generated energy spectrum, which arises from the convolution of the bremstrahlung distribution and the photon-gluon fusion cross section. Figs. 1b and 1c show the generated x_F and momentum distributions, respectively, for the charged D. The corresponding distributions for the Λ_c are similar.

III. Acceptances

Table 1 shows the acceptance for the decays $D^{\pm} \rightarrow K\pi\pi$ and $\Lambda_c \rightarrow pK\pi$ for different levels of cuts. The fractions which are not enclosed are for $50 < E_\gamma < 350$ GeV while those enclosed in parentheses are integrated only over $175 < E_\gamma < 350$ GeV. "SSD" means that the daughters of the charm decay are required to be found in the silicon strip detector by the reconstruction program. The "PWC" requirements are "SSD" plus that all daughters are found as tracks in the magnetic spectrometer. The "Cerenkov" requirements are "PWC" plus that all heavy hadrons (kaons, protons) from the decay be identified correctly: the correct identification for kaon is "K definite" or "K/p ambiguous" while that for the proton is "p definite" or "K/p ambiguous". Finally, "$\Delta z/\sigma_z > n$" consists of the "Cerenkov" requirements and that the separation in z between the decay vertex and production vertex, normalized to the uncertainty in the difference, be greater than n.

(Note on the vertexing algorithm: The simulation of tracks produced at the primary vertex is still under development in the E687 Monte Carlo program. In view of this, I chose the z of the primary vertex to be the generated position smeared by a gaussian function with σ=350 microns. This uncertainty estimated here is reasonable, perhaps even conservative, but this method of determining the primary vertex position is idealized in the sense that it ignores the tendency of tracks from secondary vertices to pull the primary vertex downstream. The determination of the secondary vertex position took into account the resolution of the silicon strip detector and multiple scattering in the target and silicon strip detector.)

From the acceptances listed in Table 1, we see that the track reconstruction and particle ID cuts account for a loss of roughly one half of the events. The effect of the vertex cuts depends strongly, as expected, on the lifetime of the charm state. After the cut $\Delta z/\sigma_z > 6$, about one-third of the charged D's and less than 10% of the Λ_c's are left. (The $<\sigma_z>$'s for the D's and Λ_c's passing the "Cerenkov" level cuts are 540 microns and 610 microns, respectively. The corresponding average momenta are 78 and 85 GeV/c, respectively. The fraction of decays passing the cut $\Delta z/\sigma_z > n$ is given roughly by $\exp\{-n<\sigma_z>/(<P>c\tau/M)\}$.)

Figure 2 shows the acceptances for various cuts in the case that the charm particle momentum or x_F is not integrated over. The acceptances after the "SSD" cuts are plotted with large diamonds, the acceptances after the "PWC" cuts with squares, the acceptances after the "Cerenkov" cuts with small diamonds, and finally the acceptances after the "$\Delta z/\sigma_z > 6$" cuts are plotted with the four-legged squares. Especially for the "Cerenkov" requirements or the "$\Delta z/\sigma_z > 6$" requirements, there is quite a bit of variation in acceptance with momentum or x_F. These plots will be discussed further in the next section.

IV. Sources of Acceptance Loss

A. Track-finding in the Silicon Strip Detector (SSD)

From inspection of Figure 2, the acceptance of the SSD and track-finding algorithm for all the charm decay products begins to fall steeply as the momentum becomes less than 50 GeV/c or as x_F becomes less than 0.25. The reason for this is geometrical: at least one of the tracks doesn't go through enough SSD planes (a minimum of 6 out of 12 is required) to be reconstructed. Figure 3a shows the momentum of such tracks in the case they are charged D daughters while Fig. 3b histograms the opening angle.

The average momentum of the missed tracks is about 4 GeV/c while the opening angles range up to 400 mr. Figure 4a is the scatter plot of the x-y projection of these tracks at approximately the position of the last SSD station, which is about 30 cm downstream of the center of the target. Were one to attempt to construct a station at that point with acceptance for most the tracks missed by the E687 SSD detector, the outer dimensions required would be something like 16x16 cm^2. (A station constructed further upstream, of course, would not have to be as large.)

Apart from tracks being outside the geometrical acceptance, one also has losses due to silicon strip inefficiencies and multiple scattering. For the states studied here, however, these losses are not very large: averaged over all possible topologies, better than 98% of the geometically accepted tracks are found.

B. Track-finding in the PWC's

As with track-finding in the SSD's, there are sizable losses at small x_F or low momentum because at least one of the charm decay daughters doesn't meet the minimum geometric requirements to be found. Let's take as minimum requirement that a track be accepted by the first magnet and two wire chambers in order to be reconstructed. (There are two magnets and five chambers, the first 3 chambers located between the two magnets and the remaining two chambers located downstream of the second. Two-chamber tracks can be found if SSD information is used.) Fig. 3c histograms the momentum of the generated charged D daughters which fail this requirement while Figure 3d is a histogram of the opening angle. The average momentum is between 3 and 4 GeV/c, and the majority of the opening angles are between 100 and 400 mr. Figure 4b is the scatter plot of the x-y projection of these missed tracks at the bend plane of the magnet.

For thinking about putting chambers in the magnets and/or changing the magnet kick in order to improve the geometric acceptance, we provide the following details about the E687 detector: (a) the first magnet plus mirror plates is about 3 m long, the bend plane about 2.3 m downstream of the target, its aperture is 38 x 63 cm^2, and the kick is 400 MeV/c vertically, (b) the first chamber has the same aperture as the magnet and is located

4 m downstream of the target, and (c) the second chamber is about 6.5 m downstream of the target and has aperture dimensions 76 x 114 cm^2.

PWC track-finding inefficiency for tracks geometrically accepted is about 4% on the average. Figure 5a shows the track-finding efficiency as a function of momentum for tracks geometrically accepted by the entire spectrometer, and Figure 5b shows the efficiency for tracks accepted through the first magnet and first three chambers. The effects of multiple scattering are manifested by the downturn in efficiency as the momentum decreases. At high momentum, the track-finding efficiency approaches 99% for fully accepted tracks and approximately 97% for tracks accepted through the first 3 chambers.

C. Particle ID with Cerenkov counters

As can be seen from Figure 2, adding particle ID cuts reduces acceptances across the board, but most striking is that beyond momenta of 100 GeV/c or x_F greater than about 0.5, the Cerenkov cuts turn the acceptance over. This last feature is mainly due to the fact that the E687 counters are gas threshold counters, although that the particle ID algorithm does not use pulse height information is also a contributing factor, in which case kaons essentially cannot be separated from pions above 62 GeV/c. Of the charged D's meeting the "PWC" requirements, 20% decay into kaons with momentum above 62 GeV/c. Obviously some of the losses are also due to misidentification or confusion in the momentum ranges where K definite, p definite, and K/p ambiguous identifications are possible. Between about 4 GeV and 62 GeV/c, for example, where perfect particle ID would return either K definite or K/p ambiguous for kaons, between 80 and 85% of the kaons from charged D decay are labeled K definite or K/p ambiguous.

D. Vertex Cuts

Acceptance of the short-lived states is clearly sensitive to the resolution between the primary and secondary vertices. In Section III above, it was noted that the average σ_z for Λ_c decays passing the tracking and particle ID cuts was 610 microns. If that could be reduced by a factor of $\sqrt{2}$ for example, the acceptance for the "$\Delta z/\sigma_z > 6$ would increase from 0.08 to about 0.14.

V. Summary

On average, after applying track reconstruction and particle ID cuts, we find the E687 acceptance for $D^{\pm} \rightarrow K\pi\pi$ or $\Lambda_c \rightarrow pK\pi$ to be about 50%. At small x_F or at large x_F, regions which are important, for example, to understanding production mechanisms, the acceptances are considerably less than that. At small x_F the relatively low acceptance is due to at least one charm daughter being outside the geometrical acceptance, while at large x_F the momentum cutoff on positive kaon ID reduces the acceptance. (To achieve high efficiency at low momentum, it is necessary not only to greatly increase the geometrical acceptance but also to find a way of positively identifying low momentum kaons and protons.)

The effect of applying vertex cuts depends strongly on the lifetime of the charmed state. For the strongest vertex cut shown, the charged D acceptance was reduced by about 25% while the acceptance for the charm baryon fell by about a factor of 6. In viewing the results of these vertex cuts, however, it must be kept in mind that this study using a very simple method for determining the error in the position of the primary vertex. Reduction of the uncertainties in the vertex positions, even by just a factor of $\sqrt{2}$, would greatly improve the acceptance for the short-lived charm states.

Table 1

Acceptances

Cut	$D^{\pm} \rightarrow K\pi\pi$	$\Lambda_c \rightarrow pK\pi$
SSD	0.79 (0.88)	0.87 (0.94)
PWC	0.64 (0.77)	0.74 (0.86)
Cerenkov	0.44 (0.44)	0.50 (0.47)
$\Delta z/\sigma_z > 3$	0.38 (0.40)	0.18 (0.21)
$\Delta z/\sigma_z > 6$	0.33 (0.35)	0.08 (0.11)

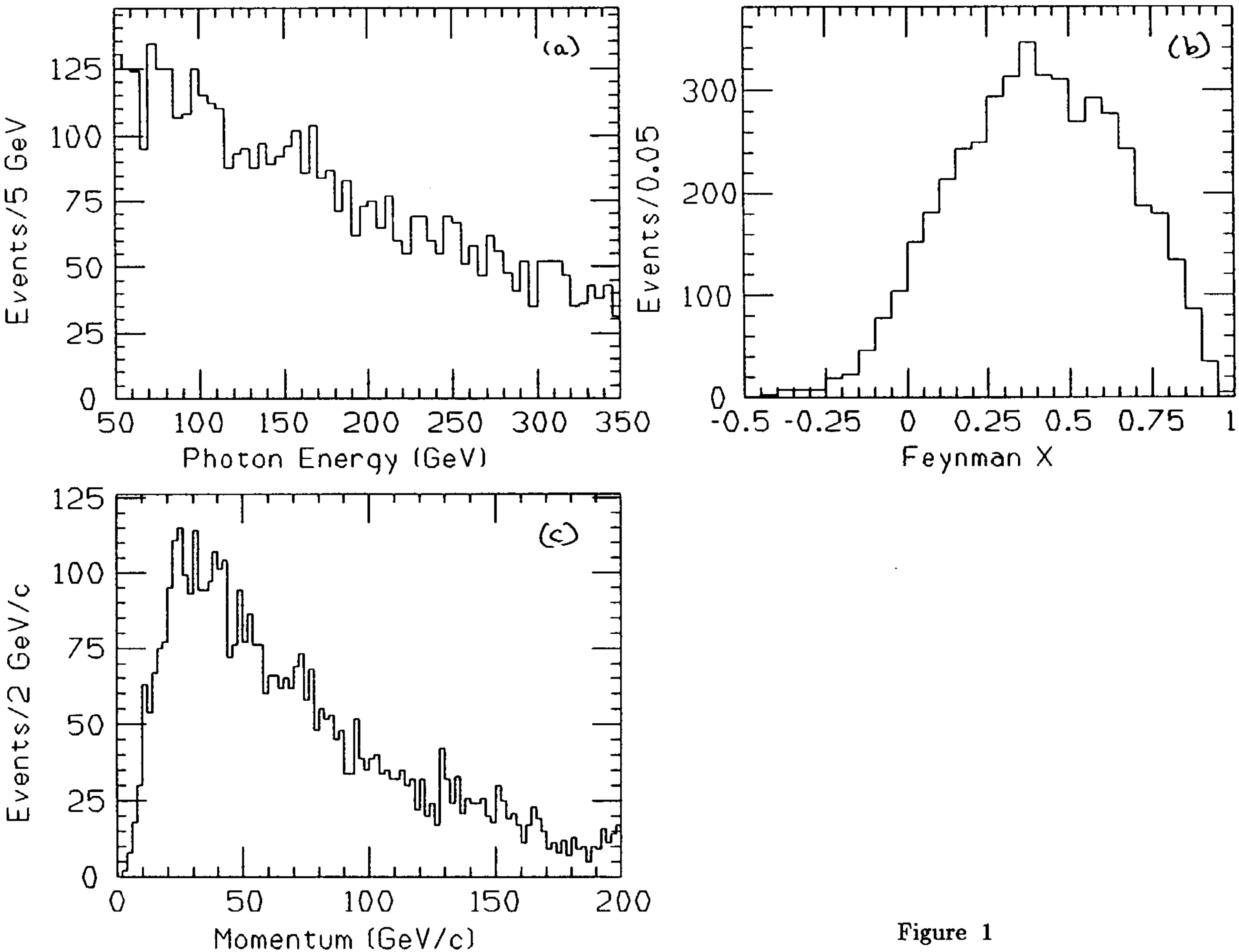

(a)
Events/5 GeV
0
25
50
75
100
125
50
100
150
200
250
300
350
Photon Energy (GeV)
(b)
Events/0.05
0
100
200
300
-0.5
-0.25
0
0.25
0.5
0.75
1
Feynman X
(c)
Events/2 GeV/c
0
25
50
75
100
125
0
50
100
150
200
Momentum (GeV/c)

Figure 1

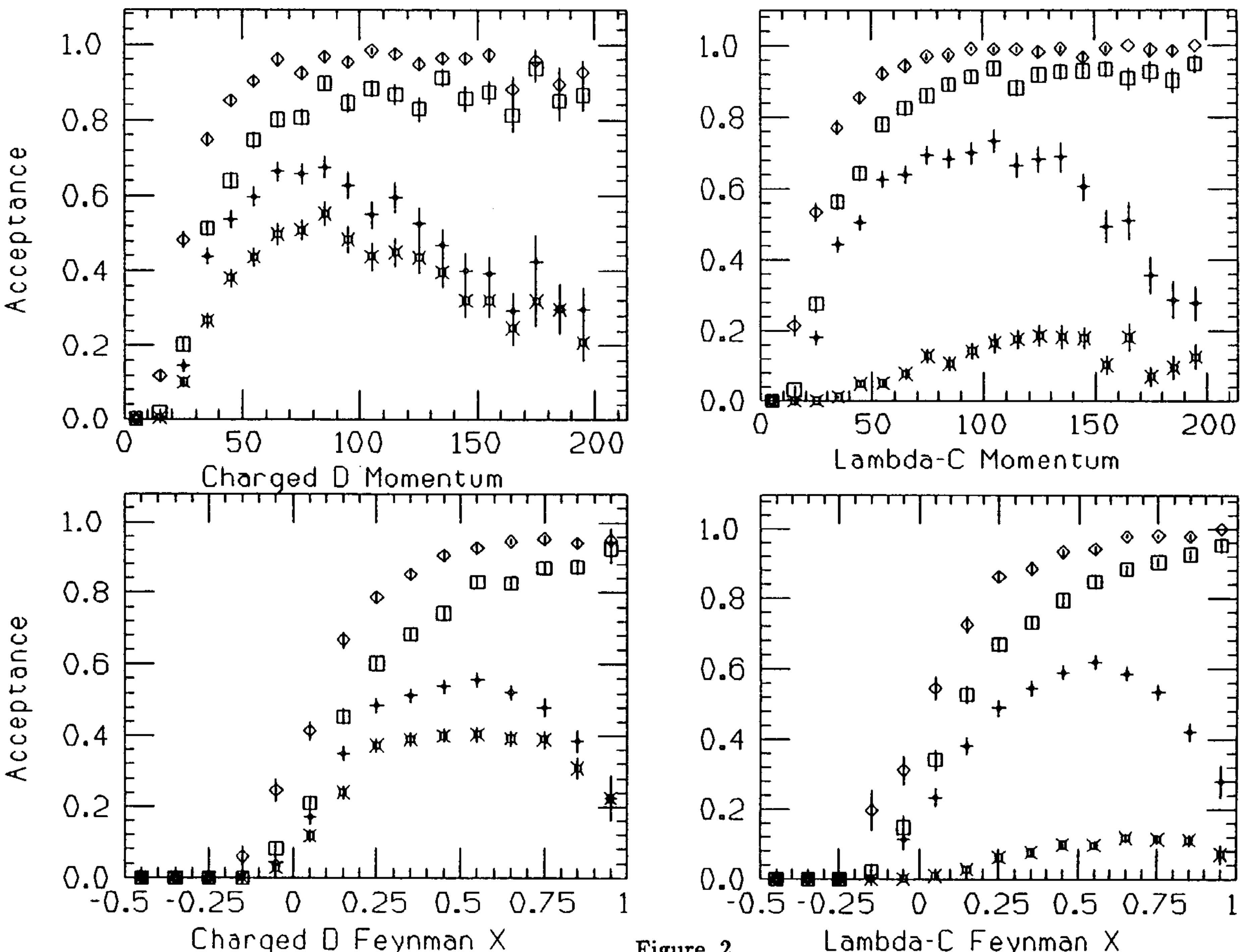

Acceptance
Charged D Momentum
Lambda-C Momentum
Acceptance
Charged D Feynman X
Lambda-C Feynman X

Figure 2

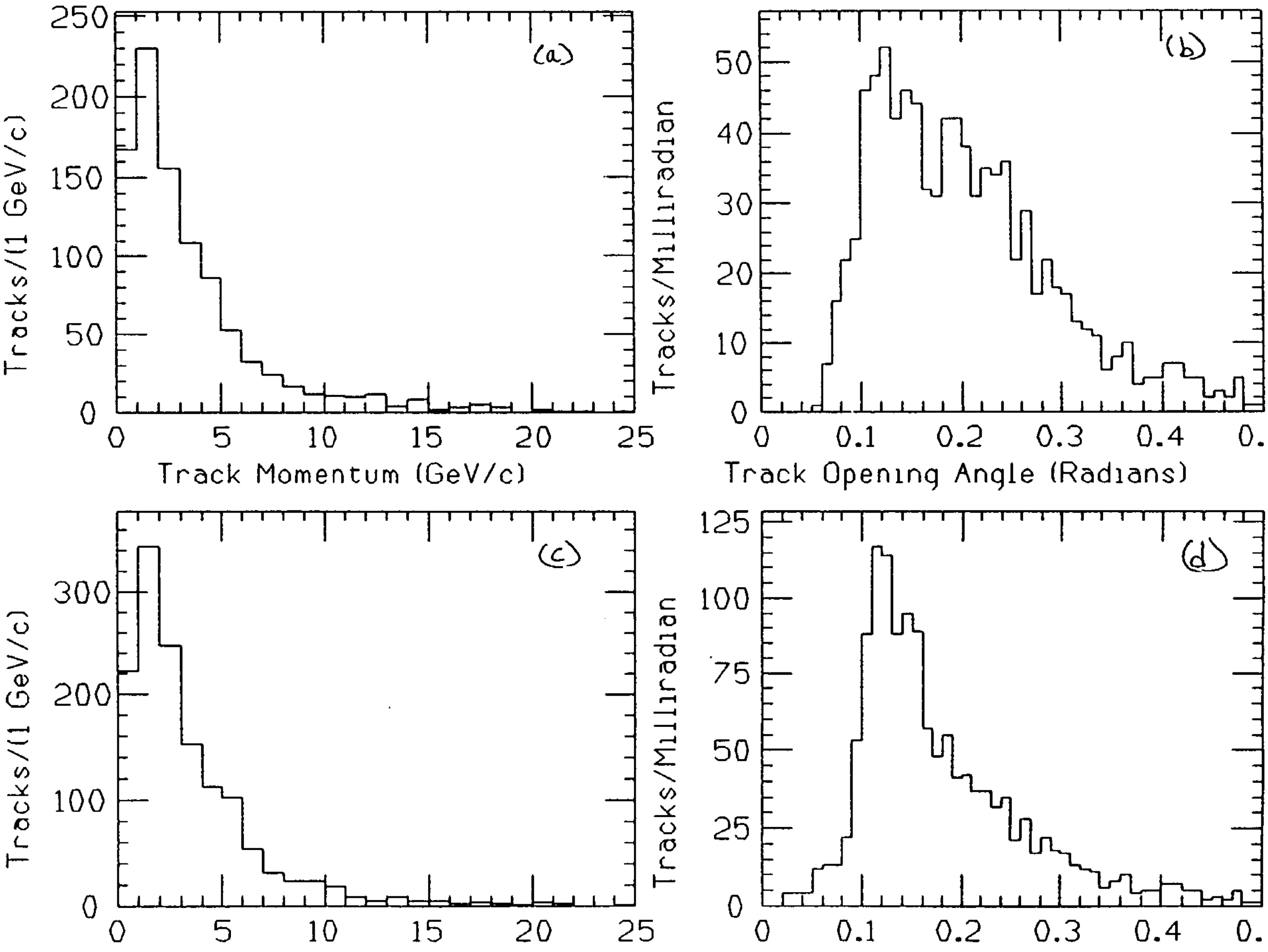
(a)
Tracks/(1 GeV/c)
Track Momentum (GeV/c)
(b)
Tracks/Milliradian
Track Opening Angle (Radians)
(c)
Tracks/(1 GeV/c)
Track Momentum (GeV/c)
(d)
Tracks/Milliradian
Track Opening Angle (Radians)

Figure 3

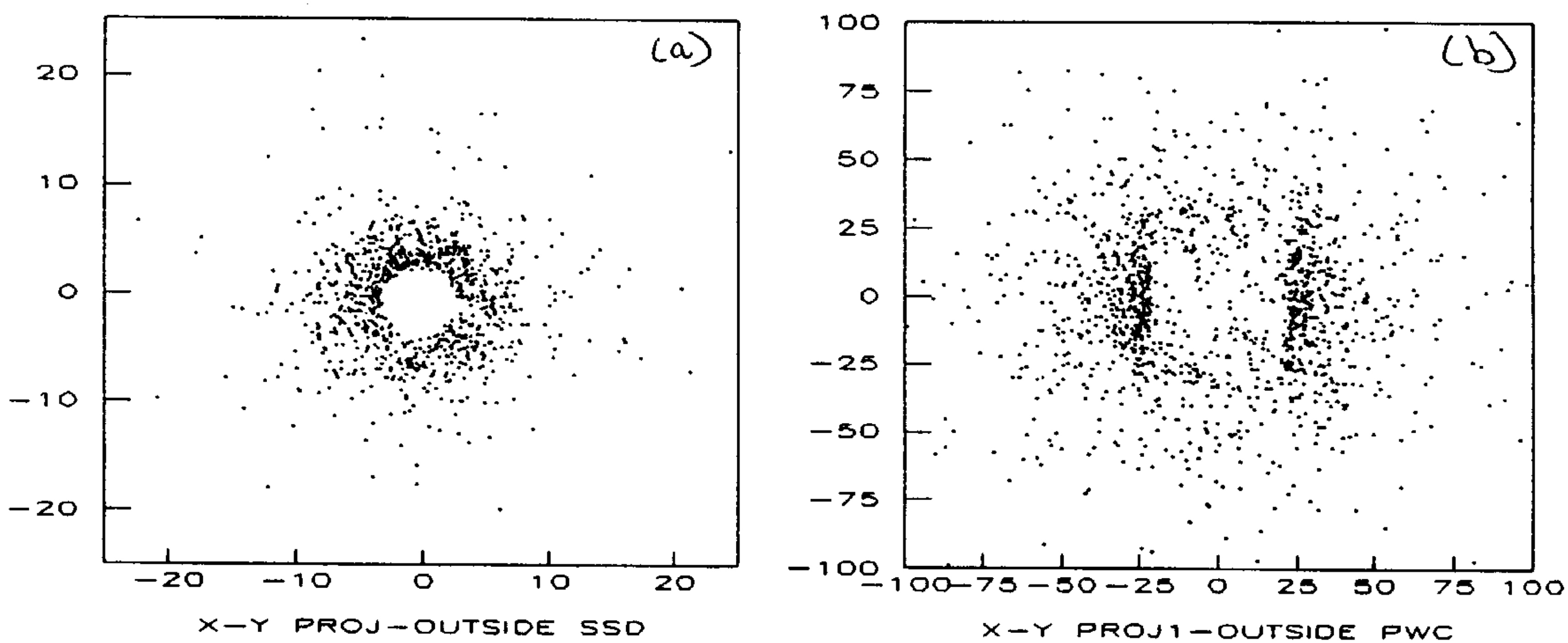

Figure 4

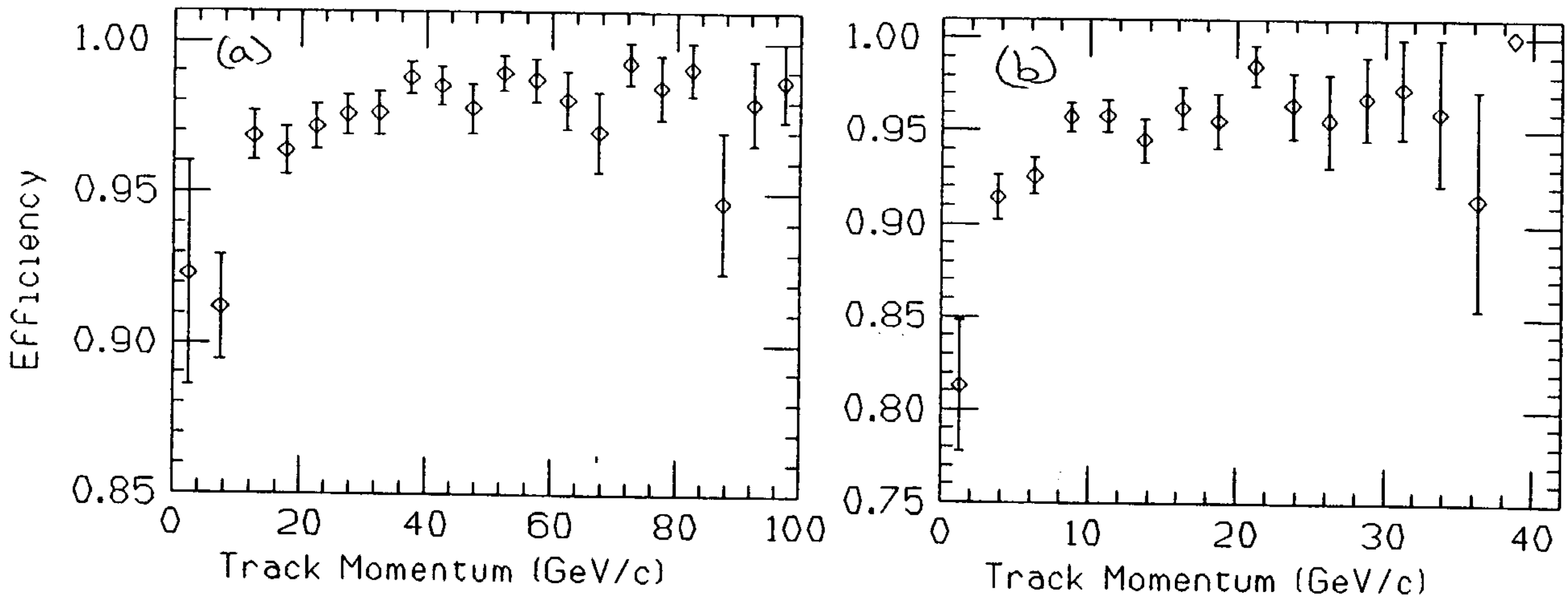
(a)
Efficiency
1.00
0.95
0.90
0.85
0
20
40
60
80
100
Track Momentum (GeV/c)
(b)
1.00
0.95
0.90
0.85
0.80
0.75
0
10
20
30
40
Track Momentum (GeV/c)

Figure 5